Magnetization reversal and chemical pressure effect in the electron doped manganite $\mathrm{CaMn_{0.95}Sb_{0.05}O_3}$

Takahiro Fujiwara, Michiaki Matsukawa,* Syuya Ohuchi and Satoru Kobayashi

Department of Materials Science and Engineering,
Iwate University, Morioka 020-8551, Japan

Shigeki Nimori

National Institute for Materials Science, Tsukuba 305-0047,Japan

Ramanathan Suryanarayanan

Laboratoire de Physico-Chimie de L'Etat Solide, CNRS,
UMR8182, Universite Paris-Sud, 91405 Orsay,France

Abstract

We have demonstrated the effect of Sr substitution on the temperature dependent magnetization reversal in the electron doped manganite $CaMn_{0.95}Sb_{0.05}O_3$. The X-ray photoemission spectroscopy reveals the substitution of Sb ion with its valence of 5+ for Mn^{4+} site, resulting in one e_g-electron doping, which is consistent with negative Seebeck coefficient previously reported. For the $(Ca_{1-y}Sr_y)Mn_{0.95}Sb_{0.05}O_3$ system, anomalously diamagnetic behaviors are observed for $y \leq 15\%$ in the weak field cooled magnetization. For the Sr content beyond 15%, the behavior of the negative magnetization disappears. We believe that the local lattice distortion due to Sb substitution causes tilting of the Jahn-Teller active $Mn^{3+}O_6$ octahedron and yields to the stabilization of the canted spin state in a opposite direction to the applied field through the Dzyaloshinsky-Moriya interaction, contributing to the diamagnetic response.

PACS numbers:

Keywords: Magnetization reversal, electron doped manganite, chemical pressure effect

---

*E-mail: matsukawa@iwate-u.ac.jp; Fax: +81-19-621-6358

I. INTRODUCTION

$CaMnO_3$, the end member of the $Ca_{1-x}La_xMnO_3$ system, undergoes a G-type antiferromagnetic transition around $T_N \sim 120$ K accompanied by a weak ferromagnetic component, [1] where each spin of Mn ions is antiparallel to its nearest neighbors of Mn. In recent years, the electron doped manganite system ($x < 0.5$) [2] has attracted much attentions because of the possibility of observing negative magnetoresistance effect like its counterpart for $x > 0.5$ in the so called hole doped manganites.

In addition to a large number of researches on the A-site substituted electron doped manganites, it has been shown that the substitution of the Mn site of $CaMnO_3$ with higher valence ions than 4+ such as $CaMn^{4+}_{1-2x}Mn^{3+}_{x}M^{5+}_{x}O_3$, with M = Nb, Ta, V, Ru, [3, 4]and $CaMn^{4+}_{1-3x}Mn^{3+}_{2x}M^{6+}_{x}O_3$, with M = Mo, W, [3,4] creates Mn^{3+} ions, i.e., electrons leading to the CMR effect. For $CaMn_{0.96}Mo_{0.04}O_3$ system, the low temperature magnetic ground state is better described by the canted AFM magnetic structure than by the phase separated state [5, 6]. It thus is interesting to examine the physical properties of the Mn-site substituted compositions for our understanding of electronic phase diagram of electron-doped manganites.

The negative magnetization phenomena in manganites have been originally reported in compounds with two sublattices of Mn ions and rare-earth ions (Nd, Gd, Dy), such as $NdMnO_3$ [7,8], (La,Gd)MnO_3, [9] (Nd,Ca)MnO_3, [10] (Gd,Ca)MnO_3, [11] and (Dy,Ca)MnO_3 [12,13]. Some of these studies were discussed on the basis of ferrimagnetic scenario leading to negative magnetization below a compensation temperature, where Mn and some rare-earths sublattices are antiferrmagnetically coupled. Moreover, a phase separation model between the ferromagnetic clusters and the canted AFM matrix is proposed, in order to account for a possible origin of the negative magnetization in manganites [7,10].

Earlier, a negative magnetization in $CaMnO_3$ with B-site substitution has been reported [14,15]. Further, we have recently demonstrated the effect of hydrostatic pressure of magnetic and transport properties, and thermal transport properties in the electron doped manganite $CaMn_{1-x}Sb_xO_3$ [16]. Anomalous magnetization reversals were clearly observed for x=0.05 and 0.08 in the field cooled magnetization while the application of external pressure induces a suppression of the negative magnetization.

In this paper, we would like to report on the influence of chemical pressure on negative magnetization of $CaMn_{0.95}Sb_{0.05}O_3$ by using the substitution of Sr with its larger ion radius for Ca site, to examine a physical role of the local lattice distortion in the magnetization reversal phenomenon.

II. EXPERIMENTS AND DISCUSSION

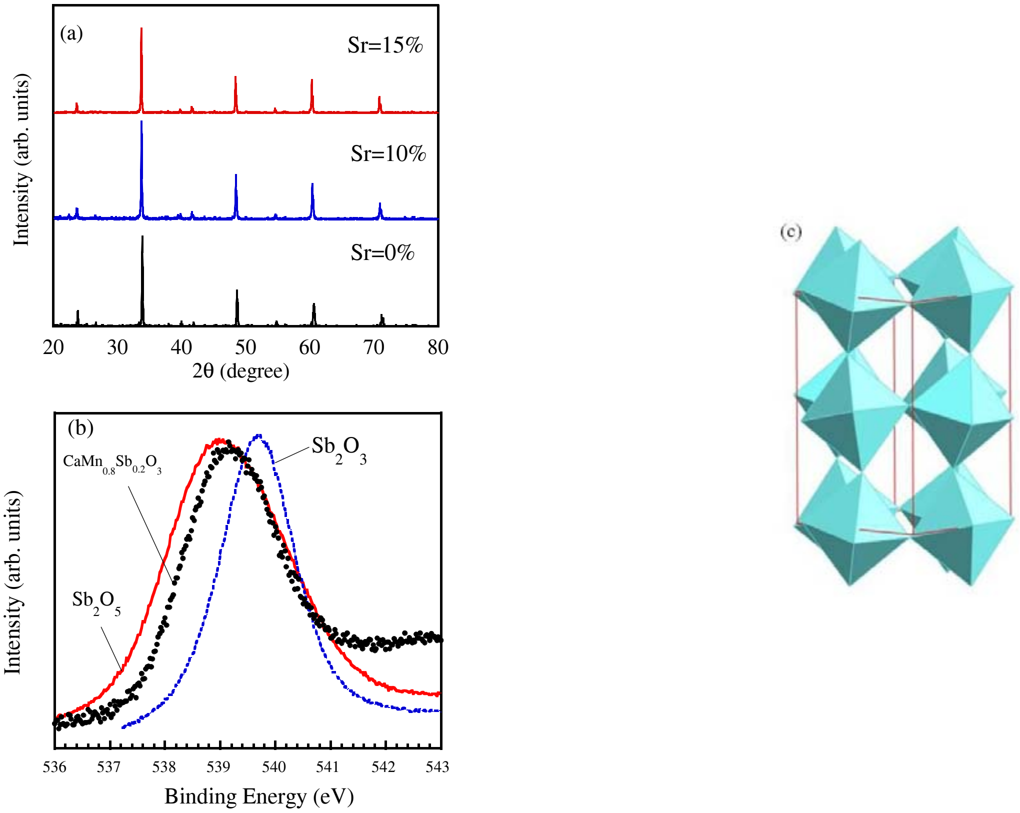

Fig. 1. (Color online)(a)X-ray diffraction patterns of $(Ca_{1-y}Sr_y)Mn_{0.95}Sb_{0.05}O_3$ (y=0.0, 0.10 and 0.15) taken at room temperature. (b) X-ray photoemission spectroscopy of $CaMn_{0.8}Sb_{0.2}O_3$. For comparison, the XPS data of both Sb_2O_3 and Sb_2O_5 powders are also given. (c) Schematic crystal structure of $CaMn_{0.95}Sb_{0.05}O_3$ with its orthorhombic distortion, arising from the connection pattern of MnO_6 octahedra.

Polycrystalline samples of $(Ca_{1-y}Sr_y)Mn_{0.95}Sb_{0.05}O_3$ (y=0.0, 0.02, 0.05, 0.10, 0.15, 0.2, and 0.4) were prepared by a solid-state reaction method. The stoichiometric mixtures of $CaCO_3$, Mn_3O_4, Sb_2O_3 and $SrCO_3$ high purity powders were calcined in air at 1000 °C for 24 h. The products were then ground and pressed into cylindrical pellets. The pellets were finally sintered at $1400 \sim 1450$ °C for 12 h. X-ray diffraction data revealed that all samples

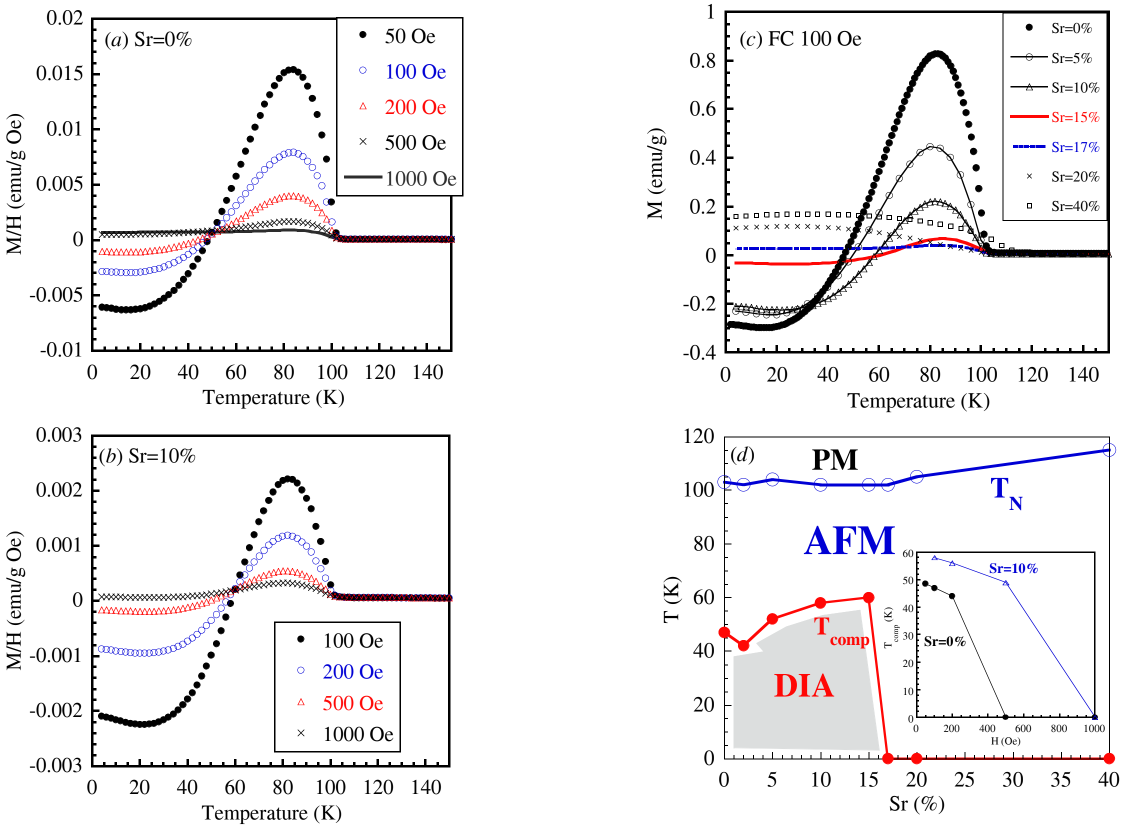

Fig. 2. (color online)(a) Field cooled (FC) magnetization curves of the parent $CaMn_{0.95}Sb_{0.05}O_3$ as a function of applied field ranging from 50 up to 1000 Oe. (b)FC magnetization curves of the Sr substituted $(Ca_{1-y}Sr_y)Mn_{0.95}Sb_{0.05}O_3$ with y=0.1. (c) FC magnetization curves of $(Ca_{1-y}Sr_y)Mn_{0.95}Sb_{0.05}O_3$ as a function of Sr content from 0 up to 40 % under 100 Oe. (d) Magnetic phase diagram of $(Ca_{1-y}Sr_y)Mn_{0.95}Sb_{0.05}O_3$. Closed and open symbols represent the compensation temperature T_{comp} crossing a zero value in M and the antiferromagnetic Néel temperature T_N, respectively. PM, AFM, and DIA denote paramagnetic, antiferromagnetic, and diamagnetic phases. The inset represents T_{comp} as a function of the applied field for the both Sr0% and Sr10% samples.

are almost single phase with orthorhombic structures ($Pnma$)(Fig.1(a) and (c)) [17]. The X-ray photoemission spectroscopy (XPS) of $CaMn_{0.8}Sb_{0.2}O_3$ (Sb20%) sample was measured at room temperature by using the Perkin-Elmer PHI-5600 system. The XPS data strongly support that the valence of Sb ion is 5+ because the XPS profile of the Sb20% sample behaves like that of Sb_2O_5 in comparison to the data of Sb_2O_3 (Fig.1(b)). The dc magnetization measurement was carried out using commercial superconducting quantum interference device

(SQUID) magnetometers both at Iwate Univ. and at the National Institute for Materials Science.

First of all, let us show in Fig.2(a) the temperature variation of the FC magnetization of the parent compound $\mathrm{CaMn_{0.95}Sb_{0.05}O_3}$ as a function of the applied field up to 1000 Oe. The magnetization reversal appears near T_{comp}=$\sim$ 47 K under low fields upon decreasing temperature. With increasing the applied field beyond 500 Oe, the behavior of negative magnetization vanishes and it is then replaced by the weak ferromagnetic tendency. To further examine the effect of local lattice distortion on the negative magnetization, we try to measure the FC magnetization of $\mathrm{(Ca_{1-y}Sr_y)Mn_{0.95}Sb_{0.05}O_3}$ (y=0.0, 0.02, 0.05, 0.10, 0.15, 0.2, and 0.4). For the Sr10% sample, a typical magnetization curve is displayed in Fig.2 (b) as a function of the applied field. The magnitude of the negative magnetization is almost invariant, but the compensation temperature T_{comp} is raised from 47 K at the parent sample up to 58 K at the Sr10% one. The negative magnetization disappears when the Sr content exceeds 15%, as shown in Fig.2(c), where the critical value y_c is estimated to be about 15 %. For the higher Sr substituted samples, their magnetization curves exhibit the weak ferromagnetic dependence over a wide range of temperatures.

In Fig.2(d), the magnetic phase diagram of $\mathrm{(Ca_{1-y}Sr_y)Mn_{0.95}Sb_{0.05}O_3}$ system is presented as a function of the Sr content. The compensation temperature T_{comp} gradually rises from 47 K to 60 K upon increasing the Sr content up to 15%, while the Néel temperature T_N=103 K remains constant ($0 \leq y \leq 0.2$). For the Sb free $\mathrm{(Ca_{1-y}Sr_y)MnO_3}$ system, the value of T_N increases from 123 K at y=0 through 130 K at y=0.1 up to 141 K at y=0.2 with the Sr content [18]. The Sr substitution for Ca site in the $\mathrm{CaMnO_3}$ matrix relaxes tilting of $\mathrm{MnO_6}$ octahedron and its associated change of the Mn-O-Mn bond angle, resulting in an increase of antiferromagnetic transition temperature T_N. However,in the electron doped case, there exists the Jahn-Teller (JT) type orbital lattice coupling between $3d$ e_g electron and $\mathrm{Mn^{3+}O_6}$ octahedron. In particular, the $\mathrm{Sb^{5+}}$ substitution with its larger ion radius for Mn site affects the neighboring $\mathrm{Mn^{3+}O_6}$, resulting in the variation of the orbital state of the e_g electron through the local JT effect.

Here, we assume that the appearance of negative magnetization due to the Sb substitution is stabilized by a canted spin state in an opposite direction to the applied field through the Dzyaloshinsky-Moriya (DM) interaction. If the substitution of Sr for Ca site gives rise to a relaxation of local lattice distortion around $\mathrm{Sb^{5+}O_6}$, we then expect a suppression of canted spin configuration contributing to the negative magnetization. In addition to it, the tilting of $Mn^{4+}O_6$ octahedron without the JT active ion is relaxed by introducing the larger Sr ion as mentioned above. The magnetization peak below Néel temperature is substantially depressed from 0.8 emu/g at y=0 down to 0.2 emu/g at y=0.1 with the Sr content. This finding is probably explained by a decrease of the positive canted magnetic component associated with a suppression of the tilting of $Mn^{4+}O_6$ octahedron [18]. The Sr substitution for A site influences more strongly the $Mn^{4+}O_6$ major region ($\sim$ 90%)with the canted AFM state contributing to positive magnetic component, in comparison to its effect on minor region ($\sim$ 10%) of a canted spin state in a direction opposite to the applied field around both $Sb^{5+}O_6$ and $Mn^{3+}O_6$ octahedra. Here, the occupation fraction of B site is estimated by using the formula $CaMn^{4+}_{1-2x}Mn^{3+}_xSb^{5+}_xO_3$ with x=0.05. Accordingly, it is reasonable that the diamagnetic response is observed up to higher Sr content of 15%.

III. SUMMARY

We have demonstrated the chemical pressure resulting from the Sr substitution in the electron doped manganite $CaMn_{0.95}Sb_{0.05}O_3$ suppresses the negative magnetization observed in the parent compound and induces a reversal in magnetization. The X-ray photoemission spectroscopy gives an experimental evidence for the substitution of Sb^{+5} ion for Mn^{4+} site, resulting in one electron doping into Mn site. The behavior of negative magnetization disappears when the Sr content exceeds 15%. The magnetization reversal phenomenon of this system is not explained by ferrimagnet model because of the absence of magnetic ion at A site. We believe that the local lattice distortion due to Sb substitution causes tilting of the Jahn-Teller active $Mn^{3+}O_6$ octahedron and yields to the stabilization of the canted spin state in a opposite direction to the applied field through the Dzyaloshinsky-Moriya interaction, contributing to the diamagnetic response.

ACKNOWLEDGMENTS

The authors thank K. Kobayashi for his assistance in XPS experiment at Center for Regional Collaboration in Research and Education, Iwate University.

REFERENCES

[1] J. B. MacChesney, H. J. Williams, J. F. Potter and R. C. Sherwood, Phys. Rev. **164**, 779 (1967).

[2] H. Chiba, M. Kikuchi, K. Kasuba, Y. Muraoka and Y. Syono, Solid State Commun. **99**, 499 (1996).

[3] B. Raveau, Y. M. Zhao, C. Martin, M. Hervieu, and A. Maignan, J. Solid State Chem. **149**, 203 (2000).

[4] L. Pi. S. Hebert, C. Martin, A. Maignan, and B. Raveau, Phys. Rev. **B67**, 024430 (2003).

[5] E. Rozenberg, M. Auslender, A. I. Shames, C. Martin, and S. Hebert, J. Appl. Phys. **103**, 07F720 (2008).

[6] C. Martin, M. Miclau, S. Hebert, M. Giot, A. Maignan, G. Andre, and F. Bouree-Vigneron, J. Magn. Magn. Mater. **321**, 3938 (2009).

[7] F. Bartolome, J. Herrero-Albillos, L. M. Garcia, J. Bartolome, N. Jaouen and A. Rogalev, J. Appl. Phys. **97**, 10A503 (2005).

[8] I. O. Troyanchuk, V. A. Khomchenko, S. N. Pastushonok. O. A. Novitsky, V. I. Pavlov and H. Szymczak, J. Magn. Magn. Mater. **303**, 111 (2006).

[9] J. Hemberger, S. Lobina, H. A. Krug von Nidda, N. Tristan, V. Yu. Ivanov, A. A. Mukhin, A. M. Balbashov and A. Loidl, Phys. Rev. **B70**, 024414 (2004).

[10] I. O. Troyanchuk, V. A. Khomchenko, G. M. Chobot, A. I. Kurbakov, A. N. Vasilev, V. V. Eremenko, V. A. Sirenko, M. Yu. Shvedun, H. Szymczak and R. Szymczak, J. Phys. Condens. Mater. **15**, 8865 (2003).

[11] O. Pena, M. Bahout, K. Ghanimi, P. Duran, D. Gutierrez and C. Moure, J. Mater. Chem. **12**, 2480 (2002)

[12] C. A. Nordman, V. S. Achutharaman, V. A. Vasko, P. A. Kraus, A. R. Ruosi, A. M. Kadin and A. M. Goldman, Phys. Rev. **B54**, 9023 (1996).

[13] M. Mouallem-Bahout, O. Pena, D. Gutierrez, P. Duran and C. Moure, Solid State Commun. **122**, 561 (2002).

[14] R. Ang, Y. P. Sun, Y. Q. Ma, B. C. Zhao, X. B. Zhu and W. H. Song, J. Appl. Phys. **100**, 063902 (2006).

[15] Y. Murano, M. Matsukawa, S. Kobayashi, S. Nimori and R. Suryanarayanan,Journal of Physics. Conf. Series **200**, 012114 (2010).

[16] Y. Murano, M. Matsukawa, S. Ohuchi, S. Kobayashi, S. Nimori, R. Suryanarayanan, K.

Koyama and N. Kobayashi, Phys. Rev. **B83**, 054437 (2011).

[17] V. Poltavets, K. Vidyasagar and M.Jansen, J. Solid State Chem. **177**, 1285 (2004).

[18] O. Chmaissem, B. Dabrowski, S. Kolesnik, J. Mais, D. E. Brown, R. Kruk, P. Prior, B. Pyles and J. D. Jorgensen, Phys. Rev. **B64**, 134412 (2001).